



FEDERAL UNIVERSITY OF SANTA CATARINA
TECHNOLOGICAL CENTER
DEPARTMENT OF MECHANICAL ENGINEERING
MATERIALS ENGINEERING PROGRAM

Lucas Teruo Hoga

Screw-Based Additive Manufacturing in Pure Alumina

Florianopolis

2024

Lucas Teruo Hoga

Screw-Based Additive Manufacturing in Pure Alumina

Final Year Project submitted to the Materials Engineering Program of the Technological Center at the Federal University of Santa Catarina as a partial requirement for obtaining the title of Bachelor in Materials Engineering.
Advisor: Prof. Rodrigo Perito Cardoso
Co-advisor: Prof. Dachamir Hotza

Florianopolis

2024

Hoga, Lucas Teruo
Screw-Based Additive Manufacturing in Pure Alumina /
Lucas Teruo Hoga ; orientador, Rodrigo Perito Cardoso,
coorientador, Dachamir Hotza, 2024.
47 p.

Trabalho de Conclusão de Curso (graduação) -
Universidade Federal de Santa Catarina, Centro Tecnológico,
Graduação em Engenharia de Materiais, Florianópolis, 2024.

Inclui referências.

1. Engenharia de Materiais. 2. Additive Manufacturing.
3. Technical Ceramics. 4. Void Defects. 5. High solid
loading. I. Cardoso, Rodrigo Perito. II. Hotza, Dachamir.
III. Universidade Federal de Santa Catarina. Graduação em
Engenharia de Materiais. IV. Título.

Lucas Teruo Hoga

Screw-Based Additive Manufacturing in Pure Alumina

This Final Year Project has been deemed suitable for obtaining the Bachelor's degree and approved in its final form by the Materials Engineering Program.

Location: Florianopolis, July 12, 2024

[Empty dotted box for signature]

Course Coordination

Examination Board

[Empty dotted box for signature]

Prof.(a) Rodrigo Perito Cardoso, Dr.(a)

Advisor(a)

[Empty dotted box for signature]

Felipe Gonçalves Jedy, Dr.(a)

Federal University of Paraná

[Empty dotted box for signature]

Guilherme Seiti Kobayashi, Me.(a)

Federal University of Paraná

Florianopolis, 2024.

This work is dedicated to my parents,
who took me to pottery classes in my
youth and taught me the Wonders of
Craftsmanship.

ACKNOWLEDGMENTS

I would like to thank the Federal University of Santa Catarina for providing the resources, facilities, and environment essential to my academic journey. The infrastructure from LABMAT and the equipment and materials from CERMAT have been invaluable in conducting this research.

I extend my heartfelt thanks to my advisor, Prof. Rodrigo Perito Cardoso, for his guidance and patience. Your support has been crucial to finish this research. I am also deeply grateful to my co-advisor, Prof. Dachamir Hotza, for his valuable insights and encouragement for my further academic path.

A special thanks to my research group, Fernando Irto Zanetti, Gustavo Alves Lau and Guilherme Seiti Kobayashi for their continuous support, advice, and assistance.

I would like to thank Prof. Marcio Celso Fredel and Prof. João Batista Rodrigues Neto for the intriguing courses in technical ceramics and for highlighting the possibilities and wonders that make the pursuit of knowledge in advanced ceramics a worthwhile subject to explore.

I would also like to thank the university restaurant, the "RU", for providing sustenance and making my stay at UFSC more manageable. Your services have been an essential part of my daily life and have contributed to my overall well-being during this journey.

ABSTRACT

Additive manufacturing (AM) has presented as a disruptive approach for the production of complex geometries and custom-made components across various industrial sectors. This study examines the extrusion-based AM of alumina parts using a 58%vol high solid loading feedstock. The goal is to investigate the influence of extrusion flow parameters on void defects and dimensional accuracy. Utilizing a screw-based extruder, different flow rates were evaluated for their effects on void formation, surface irregularities, and sintered part quality. The feedstock is composed of alumina powder and a multi-component binder system. Characterization involved Scanning Electron Microscopy (SEM) to analyze internal structures and quantify void defects. The findings indicate that increasing extrusion flow reduces dimensional deviation and void size. This research provides insights into optimizing extrusion AM processes to enhance the performance and reliability of ceramic components.

Keywords: additive manufacturing; screw-based extruder; voids; flow rate; advanced ceramics; alumina

RESUMO

A manufatura aditiva (AM) tem se apresentado como uma abordagem disruptiva para a produção de geometrias complexas e componentes personalizados em vários setores industriais. Este estudo foca na AM baseada em extrusão de peças de alumina usando uma carga sólida alta de 58% em volume. O objetivo é investigar a influência dos parâmetros de fluxo de extrusão sobre a geração de vazios e a precisão dimensional. Utilizando um extrusor de fuso, diferentes taxas de fluxo foram avaliadas quanto aos seus efeitos na formação de vazios, irregularidades de superfície e qualidade das peças sinterizadas. O feed stock é composto por pó de alumina e um sistema de aglutinantes multicomponentes, foi caracterizado usando Microscopia Eletrônica de Varredura (SEM) para analisar estruturas internas e quantificar defeitos de vazios. Os resultados mostram que o aumento do fluxo de extrusão reduz a desvio dimensional e o tamanho dos vazios. Esta pesquisa fornece insights para a otimização dos processos de AM por extrusão, visando melhorar o desempenho e a confiabilidade dos componentes cerâmicos.

Palavras-chave: manufatura aditiva; extrusor de rosca; vazios; taxa de fluxo; cerâmicas avançadas; alumina

LIST OF FIGURES

Figure 1 - Feedstock microstructure structure throughout processing steps	19
Figure 2 - Injection molding process flow	20
Figure 3 - CAD object converted to STL format in different STL resolution .	22
Figure 4 - illustration of conversion of STL format to a sliced object	22
Figure 5 - Filament-Based extruder schematics.....	23
Figure 6 - Filament-fracture due to shear stress	25
Figure 7 - Screw-Based extruder schematics	26
Figure 8 - Sample's Geometry.....	30
Figure 9 - Illustration of flow groups	32
Figure 10 - Lömi EBA series	34
Figure 11 – Sample prepared for SEM.....	36
Figure 12 – Regions containing voids from adjacent deposition	36
Figure 13 – Dimensional deviation in horizontal axis	37
Figure 14 – Sample shrinkage in different sintering temperatures	38
Figure 15 – SEM in different flow conditions	39
Figure 16 – Defect threshold identification from SEM image.....	40
Figure 17 – Void Area in different flow conditions	41
Figure 18 – Sintered surface.....	42

LIST OF TABLES

Table 1 - Feedstock Constitution	29
Table 2 - Printing parameters.....	31
Table 3 - Sample's flow arrangement.....	33
Table 4 - Sample Firing planning	35

LIST OF ABBREVIATIONS AND ACRONYMS

AM	Additive manufacturing
SEM	Scanning Electron Microscope
CAD	Computer-Aided Design
STL	Standard Tessellation Language
ABS	Acrylonitrile Butadiene Styrene
PLA	Polylactic Acid
PC	Polycarbonate
PA	polyamide
PW	paraffin wax

TABLE OF CONTENTS

1	INTRODUCTION.....	16
1.1	GENERAL OBJECTIVE	17
1.2	SPECIFIC OBJECT	17
2	LITERATURE REVIEW	18
2.1	FEEDSTOCK COMPOSITION AND PROCESSING	18
2.2	INJECTION MOLDING.....	19
2.2.1	Advantages.....	20
2.2.2	Disadvantages	21
2.2.3	Comparison with Additive Manufacturing.....	21
2.3	ADDITIVE MANUFACTURING	21
2.3.1	Concept	21
2.3.2	Slicing.....	22
2.4	EXTRUSION AM	23
2.4.1	Material extrusion of filaments	23
2.4.2	Disadvantages of Feedstock in shape of Filament	24
2.5	MATERIAL SCREW-BASED EXTRUSION.....	25
2.5.1	Concept	25
2.5.2	Screw-Based Extruder Advantages	26
2.5.3	Screw-Based Extruder disadvantages	27
2.6	ADVANCED CERAMICS.....	27
2.6.1	Alumina	28
2.6.2	Importance of Defect-Free Technical Ceramics Components.....	28
3	MATERIALS AND METHODS	29
3.1	FEEDSTOCK PRODUCTION.....	29
3.2	PRINTING PROCEDURE	30
3.2.1	Slicing Setup	30
3.2.2	Printer Settings.....	31
3.3	SAMPLE PRODUCTION.....	32
3.4	GREEN BODY MEASUREMENTS	33
3.5	CHEMICAL DEBINDING	33
3.6	THERMAL DEBINDING	34
3.7	SINTERING	34
3.8	SAMPLE CHARACTERIZATION	35

3.8.1	Dimensional Shrinkage.....	35
3.8.2	Scanning Electron Microscope.....	35
3.9	IMAGE PROCESSING.....	36
4	RESULTS AND DISCUSSION	37
4.1	GREEN BODY DIMENSIONAL ACCURACY	37
4.2	SINTERED BODY MEASUREMENTS	38
4.3	VOID DEFECTS DUE TO THE EXTRUSION AM PROCESSING	39
5	CONCLUSION	43
5.1	DIMENSIONAL ACCURACY:	43
5.2	SINTERING AND SHRINKAGE:	43
5.3	SECONDARY POROSITY AND SURFACE IRREGULARITIES:	43
5.4	FUTURE WORK.....	43

1 INTRODUCTION

Additive manufacturing has transformed how we produce complex geometries and customized components across various industrial sectors. Among the different AM techniques, Extrusion-based additive manufacturing stands out for its accessibility, versatility, and cost-effectiveness (ALTIPARMAK *et al*, 2022). This technique uses layer-by-layer deposition of material extruded through a heated nozzle, allowing the creation of intricate three-dimensional objects from digital models in a fast-processing manner. A wide range of materials, such as, polymers (LIU *et al*, 2019), metals (DUDA *et al*, 2016), composites (SINGH *et al*, 2019) and ceramics (DADKHAH *et al*, 2023) are suited to be processed in this additive manufacturing process.

Recently, there has been a growing interest in the AM of ceramics due to their mechanical, thermal, and chemical properties allied to a fast processing and freedom of shape in additive manufacturing processing (OLHERO *et al*, 2022). However, producing high-density ceramic parts using extrusion deposition is challenging, mainly due to issues related to extrusion that can lead to formation of defects such as voids. To achieve the desired properties in ceramic components, it is crucial to meticulously control the printing process of green body fabrication.

This study focuses on the AM of alumina parts from a feedstock with high solid loading using screw-based extruder technology. A significant aspect of this research is the investigation of extruder material flow parameter and its impact in the generation of void defects that are common phenomenon in the Extrusion based process. This type of void occurs in the adjacent extruded material and it can influence in the overall quality of the final ceramic parts. Scanning Electron Microscope was utilized to evaluate the internal structure, voids, and defects of the sintered samples, providing a detailed understanding of how these voids form and can be minimized.

By comparing different processing parameters and analyzing the formation of void defects, we aim to identify the optimal conditions for producing high-quality alumina parts. The findings from this study will contribute to the advancement of ceramic additive manufacturing, providing insights into optimizing screw-based processes to minimize void defects and enhance the performance of ceramic components.

The potential applications of this research span various fields, including aerospace, biomedical, and other industrial applications (BHATIA *et al*, 2023).

1.1 GENERAL OBJECTIVE

The present work aims to explore a processing technology in the segment of the of advanced ceramics components by screw-based extrusion additive manufacturing.

1.2 SPECIFIC OBJECT

Production of green alumina parts based on a polypropylene, Paraffin wax and Stearic acid multi component binder system

Processing trough debinding and sintering of alumina parts from additive manufacturing produced feedstock

Understand the influence of flow parameter and its impact in the size of void between adjacent extrusions.

2 LITERATURE REVIEW

2.1 FEEDSTOCK COMPOSITION AND PROCESSING

Injection molding is a versatile manufacturing process widely used for producing complex and high-precision components. The feedstock used in this process is critical for determining the quality and characteristics of the final product. Typically, the feedstock consists of a mixture of fine powders (either metallic or ceramic) and a multi-component binder system, which plays a vital role in shaping and debinding stages of the components manufacture.

The binder system in injection molding is composed of several essential components, each serving a specific purpose. The backbone binder provides structural integrity needed for the green parts during the initial stages of the molding process. Common materials used for backbone binders include polyethylene (PE), polypropylene (PP), and ethylene-vinyl acetate (EVA). These polymers ensure that the green parts maintain their shape and strength during handling and initial processing. (MOMENI *et al*, 2019).

The preparation of feedstock involves the thorough mixing of the powder and binder components to achieve a homogeneous mixture. This process ensures uniform distribution of the binder throughout the powder particles, which is crucial for consistent molding and subsequent processing steps. Mixing and compounding are performed using high-shear mixers or twin-screw extruders to achieve a uniform feedstock mixture with the desired rheological properties for injection molding. After mixing, the feedstock is often pelletized to facilitate feeding into the injection molding machine, achieving consistent feed rates during molding (GONZLEZ *et al*, 2012).

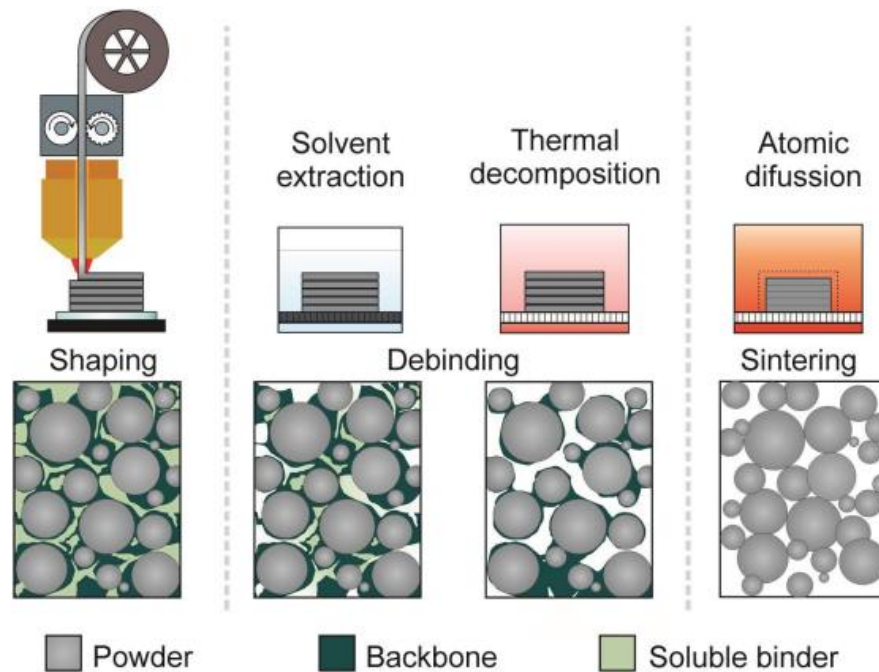
Debinding is a crucial process in the production of ceramic and metal components, where the binder used in the initial forming stage is gradually removed. Thus, solvent extraction is the first step in the debinding process, where a portion of the binder is removed to create a porous structure that facilitates the removal of the remaining binder during thermal debinding. Solvents such as hexane are commonly used. The selection of solvents is crucial as it affects the debinding rate and the integrity of the part (TUELUEMEN *et al*, 2017).

Thermal debinding follows solvent extraction and involves heating the part to remove the residual binder through thermal decomposition. This process must be

carefully controlled to prevent defects such as cracking, blistering, or distortion. Thermogravimetric analysis (TGA) is often used to optimize the thermal debinding parameters, ensuring complete binder removal without compromising the part's structure. (ZAKY, 2004)

Sintering is the final step, where the debinded parts are heated to a temperature below their melting point but high enough to cause particle bonding. This process increases the density and strength of the parts. Sintering conditions such as temperature, time, and atmosphere must be optimized to achieve the desired mechanical properties and microstructure. A dimensional shrinkage is expected to happen during sintering due to the sintered part densification (See Figure 1). (BORDIA *et al*, 2017).

Figure 1 - Feedstock microstructure structure throughout processing steps



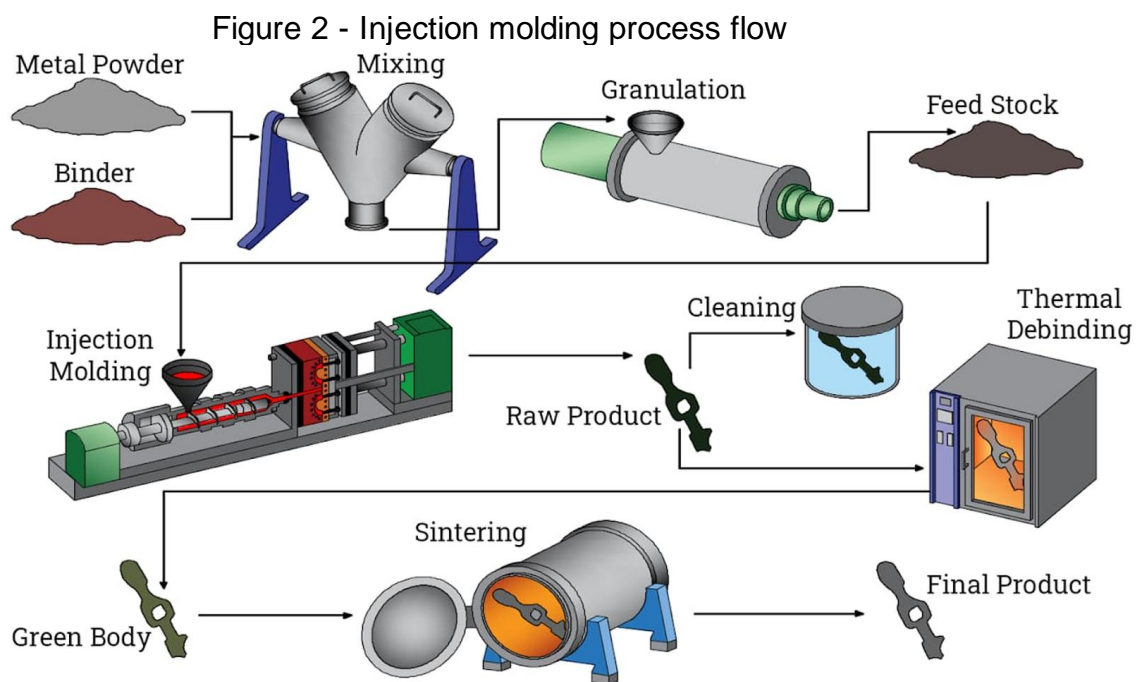
Source: (GONZALEZ *et al*, 2018)

2.2 INJECTION MOLDING

Injection molding is a widely used manufacturing process that allows for the production of components with diverse geometric shapes, high dimensional tolerance, and greater productivity compared to most competing processes. The process involves injecting molten material into a mold cavity, where it cools and solidifies into the desired

shape. This technique is commonly used for producing large volumes of identical parts with high precision. (NAKAO *et al*, 2006).

This production technique meets wide application in the field of polymeric materials due to the plasticity properties that favors the injection of polymeric materials. Also, a wide range of materials can be processed in injection molding thought the mixture of polymeric materials and the powder of materials like metals and ceramics (GONZLEZ *et al*, 2012). Figure 2 illustrates the basic processing flow for injection molding using metal powder as an example.



Source: (METAL... 2024)

2.2.1 Advantages

Injection molding features advantages such as the capacity of producing large volumes of parts in a relatively short amount of time, high dimensional accuracy and repeatability. It is versatile, suitable for complex geometries, and accommodates a wide range of materials. Additionally, it produces minimal waste, as excess material can often be recycled and reused. However, there are limitations to the process that should be considered. (ZHAO *et al*, 2020).

2.2.2 Disadvantages

Injection molding processes offer high productivity; however, the shapes of the components are constrained by the use of dies or molds, which typically have high costs. This tends to limit their application to large batches to achieve the break-even point for the cost of mold manufacturing. (ABDULLAHI *et al*, 2015).

2.2.3 Comparison with Additive Manufacturing

While injection molding is highly efficient for mass production, it is less flexible than additive manufacturing (AM) for low-volume production and customization. AM technologies, such as Fused Filament Fabrication (FFF) and Stereolithography (SLA), offer greater design freedom and the ability to produce parts on-demand without the need for molds (ACHILLAS *et al*, 2017).

2.3 ADDITIVE MANUFACTURING

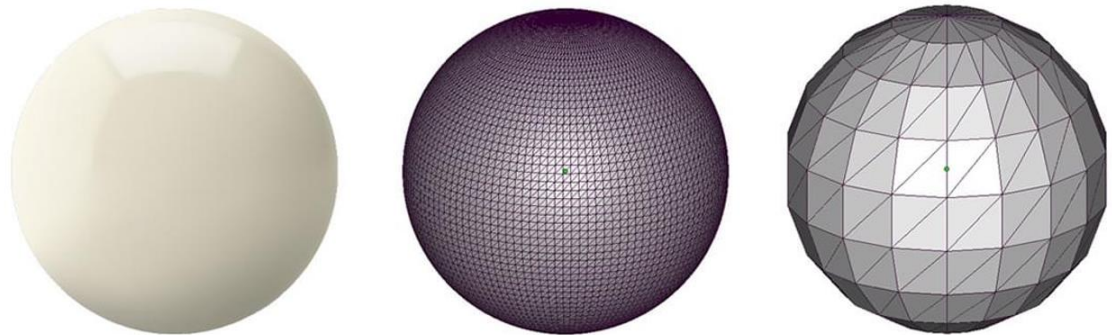
Additive Manufacturing (AM), commonly known as 3D printing, is a production approach that enables the creation of complex and precise components from digital models. This technology contrasts sharply with traditional subtractive manufacturing methods, where material is removed from a solid block to achieve the desired shape. AM builds objects layer by layer, using materials such as polymers, metals, ceramics, and composites. (GIBSON *et al*, 2009). ASTM recognizes AM as “process of joining materials to make objects from 3D model data, usually layer upon layer, as opposed to subtractive manufacturing methodologies” (ASTM, 2015)

2.3.1 Concept

Additive Manufacturing machines works by following a series of steps to convert digital models into physical objects. The specific production steps can vary depending on the type of AM technology used, but the general process begins with the creation of a 3D digital model using computer-aided design (CAD) software (GIBSON *et al*, 2009). This model serves as the blueprint for the object to be printed. The CAD

model is exported as a STL file that contains the tridimensional form of the model (See Figure 3) for then to be imported into slicing software.

Figure 3 - CAD object converted to STL format in different STL resolution



Renderized CAD Object

Refined STL 3D Object

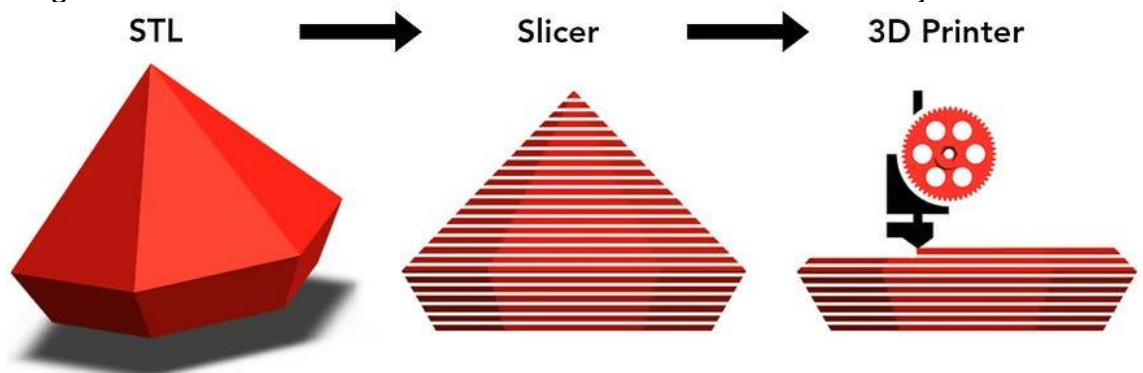
Rough STL 3D Object

Source: adapted from (FILE... 2024)

2.3.2 Slicing

The slicing stage is responsible to convert tridimensional object in two dimensional sections, which divides the model into thin horizontal layers (See Figure 4). The software generates a set of instructions (G-code) for the AM machine, detailing the path and movements needed to build each layer. (BALLETTI *et al*, 2017)

Figure 4 - illustration of conversion of STL format to a sliced object



Source: (MINTCAD 2024)

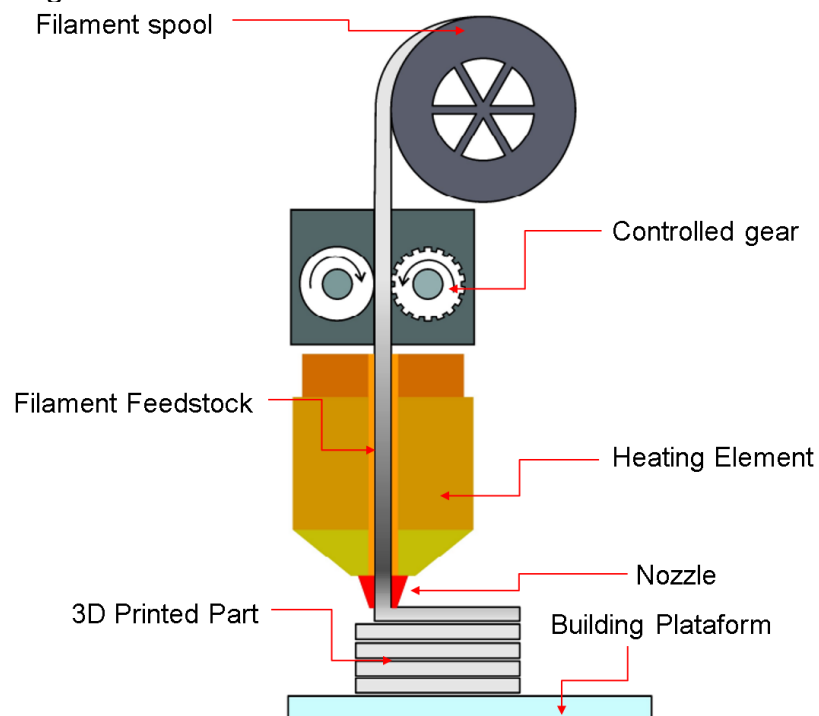
2.4 EXTRUSION AM

This section will present the different types of mechanism that an extrusion based additive manufacturing machine can operate and its main implication with the manufacturing of parts.

2.4.1 Material extrusion of filaments

This technique has become the most prevalent method in material extrusion additive manufacturing due to its straightforward and safe process. In the FFF process, a filament is fed into a heated nozzle, where it is melted and deposited layer by layer onto a building platform (See Figure 5). This platform can be heated to temperatures just below the melting point of the material to enhance adhesion and minimize thermal stress. The process is simple yet effective: the filament is first pulled by driving wheels and then pushed into a heated zone which liquefies it before being extruded through the nozzle. This requires the filament to have adequate mechanical strength to withstand the pushing force without buckling, while also being flexible enough to be spooled and fed continuously.

Figure 5 - Filament-Based extruder schematics



Source: Adapted from (Gonzalez *et al*, 2018)

The popularity of FFF is further bolstered by the wide variety of materials available in filament form. Common thermoplastics like acrylonitrile butadiene styrene (ABS) and polylactic acid (PLA) are widely used, along with other polymers such as polycarbonate (PC), polyamide (PA), and various composites. These materials can be reinforced with fibers or particles to enhance their properties.

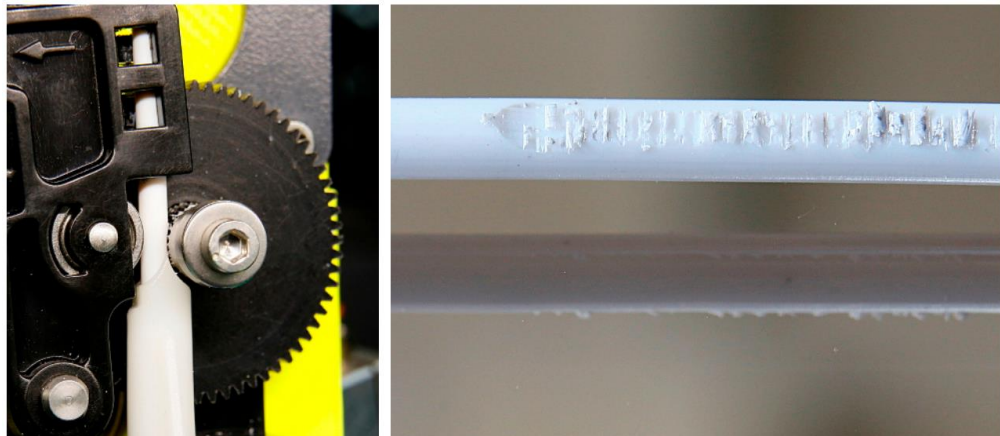
The ease of use, safety, low equipment cost, and material versatility have made FFF a dominant technique in both industrial and personal fabrication markets. This method supports the production of complex geometries and is highly adaptable for various applications, promoting innovation and customization in manufacturing (Gonzalez *et al*, 2018).

2.4.2 Disadvantages of Feedstock in shape of Filament

Fused Filament Fabrication (FFF) using as a feedstock filament presents several challenges, particularly when the solid content of the powder in the filament is high. One significant issue encountered with FFF in such conditions is the failure of the filament to extrude properly. This problem is particularly pronounced in filaments with high solid powder content, as detailed in the study by NÖTZEL *et al*, 2018.

The study highlights that when the solid content in the filament exceeds 50 vol%, the viscosity of the material increases exponentially, which severely impacts the extrudability of the filament. Specifically, filaments with a solid content of 60 vol% alumina could only be extruded manually, as the viscosity was too high for the printer's extruder to handle. This high viscosity leads to grinding at the filament surface as the extruder gear is unable to move the filament, thereby causing extrusion failure. Figure 6 displays the filament grinded failure at the surface due to high solid loading content. This is a significant disadvantage because it limits the efficiency and reliability of the FFF process for producing parts with high solid content (NÖTZEL *et al*, 2018).

Figure 6 - Filament-fracture due to shear stress



Source: (NÖTZEL *et al*, 2018)

2.5 MATERIAL SCREW-BASED EXTRUSION

The production of filaments for fused filament fabrication (FFF) machines requires specialized extrusion lines and expertise processing control to achieve a constant cross-sectional area and minimal ovality. This precision is essential for depositing the correct amount of material and ensuring a reliable process via FFF. Also, not all materials for binder mixtures can be made into filaments that are both spooled and carry a high amount of powder loading to be pushed by FFF feeding mechanisms. Consequently, several research groups and companies are exploring screw-extrusion additive manufacturing (AM) machines that can utilize pellets (CURMI *et al*, 2022).

2.5.1 Concept

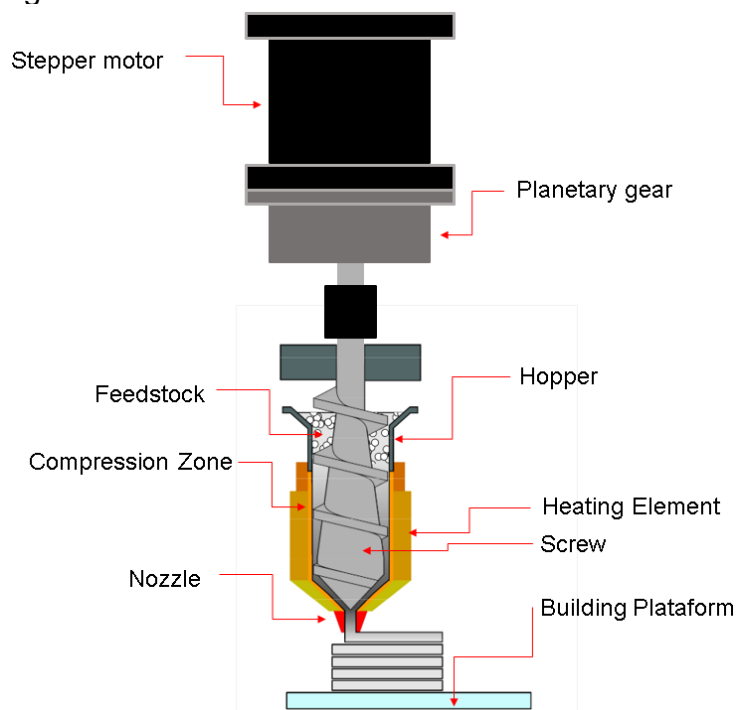
Screw-based extruders are essential to the advancement of additive manufacturing, especially when working with highly filled polymeric composites and metal matrix composites. The key component of a screw-based extruder is the rotating screw, which performs multiple critical functions: transporting, compressing and plasticizing the feedstock material.

In the feed zone, the primary function is to transport the pellets from the hopper into the extruder (See Figure 7 at hopper). The screw's rotation moves the material forward while the deep flights (spaces between the screw threads) allow a large volume of material to be introduced.

As the material progresses into the compression zone (See Figure 7), the flight depth decreases, which compresses the material and starts the plasticization process. The friction and heat generated from the compression and shear forces help melt the feedstock. The screw's design in this zone ensures thorough mixing and homogenization of the material, which is crucial for maintaining consistent material properties. The barrel surrounding the screw is equipped with heating elements (See Figure 7) that precisely control the temperature along the length of the extruder.

Finally, the homogenized and pressurized material is forced through a heated nozzle (See Figure 7). The nozzle's diameter determines the thickness of the extruded filament or the bead of material deposited layer by layer to form the part. The extrusion process must be carefully controlled to ensure uniform deposition.

Figure 7 - Screw-Based extruder schematics



Source: Adapted from (Gonzalez *et al*, 2018)

2.5.2 Screw-Based Extruder Advantages

One of the primary advantages of screw-based extruders is their capacity to handle a variety range of materials, including highly filled polymeric composites. This capability is especially advantageous for producing parts with a high content of ceramics or metals, which are often difficult to process using traditional filament-based

systems. The continuous feeding mechanism of the screw allows for the use of feedstock in form of pellets or granules, significantly reducing material costs compared to pre-processed filaments. (GALANTUCCI *et al*, 2022)

2.5.3 Screw-Based Extruder disadvantages

However, there are also significant challenges associated with screw-based extruders. One major drawback is the complexity of the system, which requires careful calibration and maintenance to ensure optimal performance. The extrusion process can be sensitive to variations in material properties and processing conditions, necessitating precise control over parameters such as temperature and screw speed to avoid defects like voids or inconsistent bead formation. (LA GALA *et al*, 2021)

2.6 ADVANCED CERAMICS

Advanced ceramics are known for their exceptional properties, such as high mechanical strength, thermal resistance, electrical insulation, and chemical stability. These attributes make them essential in high-performance applications across industries like aerospace, electronics, biomedical, and energy. (ZOCCA *et al*, 2015)

Traditional manufacturing methods for advanced ceramics processing as pressing, machining and various types of casting often have significant limitations. These limitations include high costs, complex processing steps, and design constraints. This is where additive manufacturing (AM) of advanced ceramics becomes valuable, offering several compelling advantages that address these challenges and open up new possibilities. (ZOCCA *et al*, 2015), (LAKHDAR *et al*, 2021)

The customization and prototyping capabilities of AM allow for the rapid production of prototypes, enabling faster design iterations and development cycles. This is especially important in research and development, where quick testing and validation of new designs can accelerate innovation. In the biomedical field, AM facilitates the creation of highly custom-made implants and prosthetics, enhancing the fit and performance of medical devices (ZOCCA *et al*, 2015).

2.6.1 Alumina

Alumina is renowned for its high hardness, wear resistance, and mechanical strength. These properties make it ideal for applications that demand durable and robust materials, such as cutting tools, abrasives, and wear-resistant components. Its ability to maintain structural integrity under high stress and wear conditions ensures reliability and longevity in demanding environments. (MEDVEDOVSKI, 2001)

One of the significant advantages of using alumina is its cost-effectiveness. Compared to other advanced ceramics, alumina is relatively affordable, making it a practical choice for both research and industrial applications. Its availability and lower cost do not compromise its excellent properties, making it a preferred material for experiments and large-scale manufacturing (MEDVEDOVSKI, 2001).

2.6.2 Importance of Defect-Free Technical Ceramics Components

Technical ceramics are often utilized in applications where high mechanical strength and reliability are crucial. Defects such as cracks, voids, and inclusions can act as stress concentrators, drastically reducing the material's strength and making it prone to fracture under load. In high-stress applications, such as turbine blades, cutting tools, and structural components, even minor defects can lead to catastrophic failures. Ensuring that ceramic components are defect-free enhances their mechanical reliability and extends their service life (PEREIRA *et al*, 2018)

3 MATERIALS AND METHODS

3.1 FEEDSTOCK PRODUCTION

This study was done using sub micro pure alumina powder (Al_2O_3 – Alcoa/A1000). According to the manufacturer, it's average size is $0.5 \mu\text{m}$. The binder system was based on organic composition of paraffin-wax (PW), polypropylene (PP), stearic acid (SA) as surfactant and ethylene vinyl acetate copolymer (EVA) as a thickening agent. The Table 1 displays the constitution of studied feedstock. The feedstock powder loading of 58% vol had its percentage based on work done by (THOMAS-VIELMA *et al*, 2008). In this study, alumina in 58% vol obtained the best performance for processing feedstock for injection molding processing balancing solid loading, and shear rate.

Table 1 - Feedstock Constitution

Material	Mass		Vol (mL)	Volumetric Percentage (%)
	Percentage (%)	Mass (g)		
Al_2O_3	86	398,43	100,9	58,0
SA	0,65	3,04	3,0	1,7
PW	5,23	24,35	27,1	15,6
PP	6,19	28,83	30,3	17,5
EVA	2,40	11,16	12,4	7,1
Anti Ox	0,04	0,17	0,2	0,1
Total	100	465,99	173,9	100,00

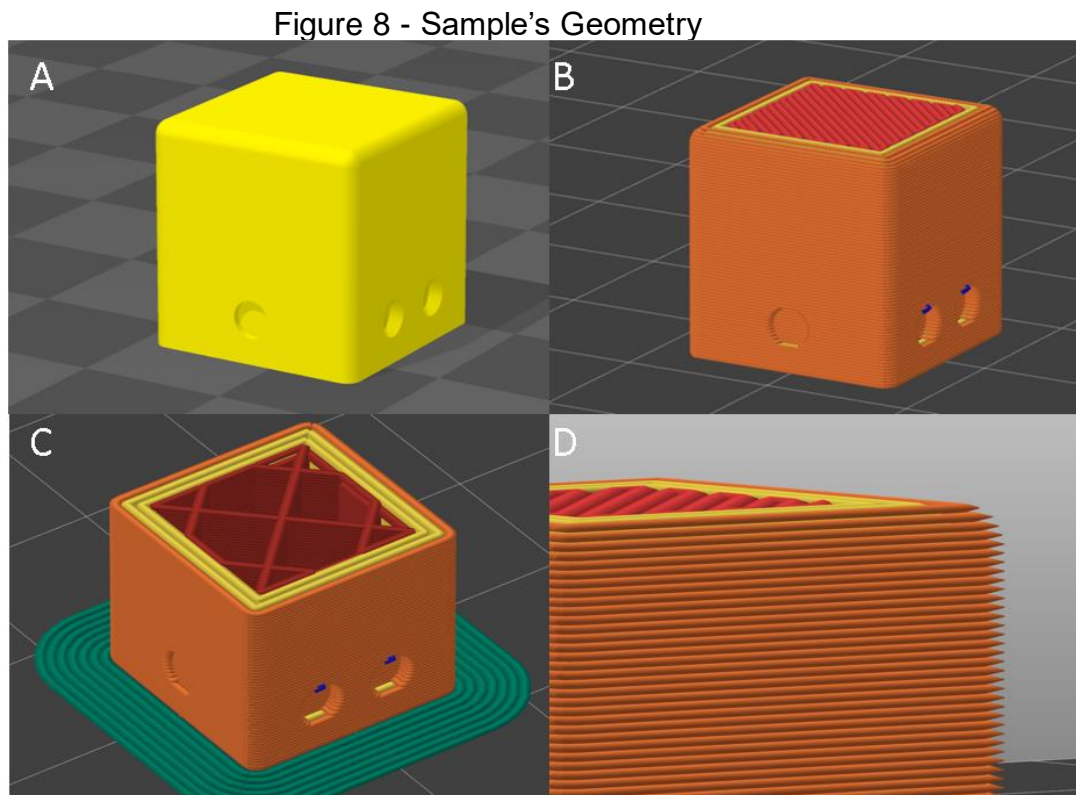
Source: Authors own authorship.

The feedstock was pre mixed in a 1000 mL beaker, combining alumina powder and binder components in pellet form. The mixing process took place using a Haake Sigma mixer set at 170°C in 70 rpm for 60 minutes. After this period, the mixed feedstock as a paste aspect was spread onto a metallic smooth surface and cut into small pieces while still hot to facilitate processing in a crusher. The feedstock was then grounded in a knife grinder and subsequently separated into a powder ranging between $180 < \varnothing < 500 \mu\text{m}$.

3.2 PRINTING PROCEDURE

3.2.1 Slicing Setup

The testing geometry was set as a cube of dimensions as 15 X 15 X 15 mm featuring small circles in the X axis (two circles) and Y axis (one circle). The Prusa Slicer program was used to generate the G-code file. The sample's illustration can be observed in Figure 8A before slicing. Figure 8B displays features such as Perimeter (yellow), External Perimeter (orange), Overhang Perimeter (blue), Top Solid infill (red) of a sliced version. Figure 8C displays the Internal infill feature in a grid pattern, Figure 8D shows in more details the aspect of deposited layers on the external perimeter consideration for the end printed part.



Source: Authors own authorship.

Details related to printing parameter settings are shown in Table 2.

Table 2 - Printing parameters

Layer height	0.2mm
Nozzle diameter	0.6mm
Perimeters/Wall	3
Top solid layers	3
Bottom solid layers	2
Infill	25%
Infill pattern	Grid
Volumetric Speed	1mm ³ /s
Printing speed	8mm/s
¹ Filament diameter	1.75mm
Extrusion multiplier	1
Printing Nozzle temperature	220°C
Printing bed temperature	100°C

Source: Authors own authorship.

After the setup in complete Slicer program generate a G code featuring all configuration for the 3D printer to run. The G code file was stored in a micro-SD device.

3.2.2 Printer Settings

The extruding parameter for the additive manufacturing machine was referenced from the extruder head manufacturer's specifications, which recommend a screw rotation setting of 450 steps/mm for extruding Polylactic Acid (PLA) polymer. This setting was used as a baseline for the experiment, representing 100% flow rate.

A Creality 0.6mm nozzle was employed in this study, as referenced by (HEIM *et al*, 2023). Attempts to use a smaller nozzle size, such as 0.4mm, resulted in unreliable outcomes due to clogging during the printing process.¹

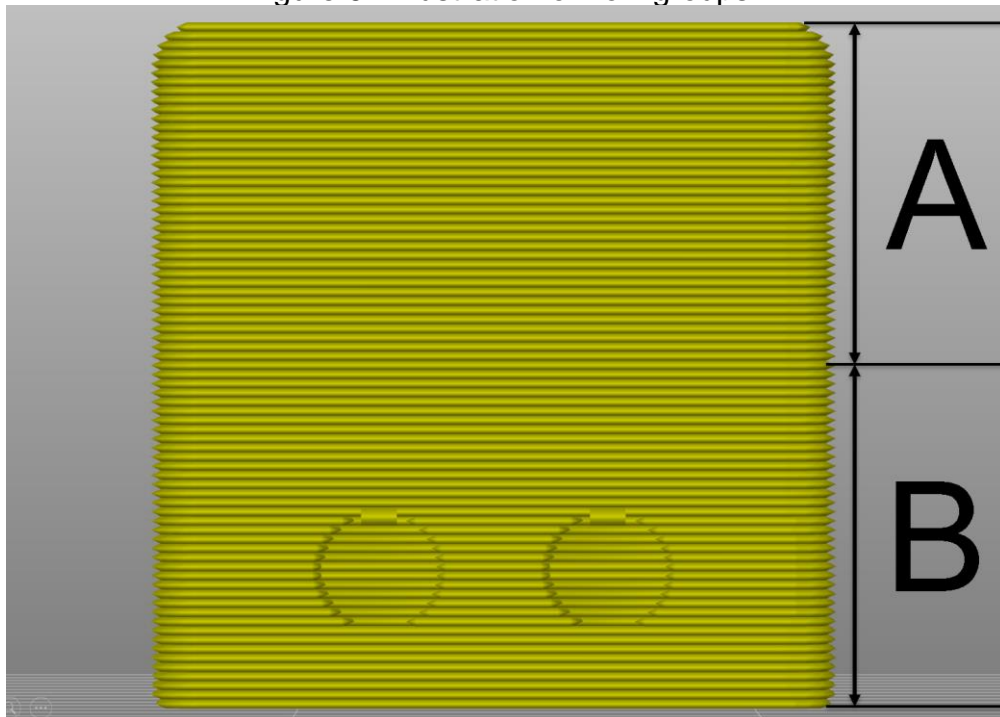
1. The printer needs a value for extruder intake diameter, despite the experiment setup used a screw extruder. The value of 1.75 mm is a common filament diameter available in the market and the standard diameter for most filament feed 3D printers.

3.3 SAMPLE PRODUCTION

The printing procedure was done using a modified Creality Ender 5 PRO equipped with a Mahor V4 pellet extruder. The printer's hot end and bed were preheated to ensure proper printing preparation. After the end of preheating cycle, the micro-SD card containing G-code file was inserted in the printer, and the sample's file was sent to print.

The flow parameters varied from 80% to 100%. Each sample carried two flow conditions. As the printer's panel indicated the current printing height, the flow was adjusted manually from the printer panel at the sample's middle height in increment of 5%. Samples with different flow conditions were referred as flow samples. Flow samples were organized in two groups, representing the flow conditions in different coordinates used in each sample batch. The upper flow condition was referred as group A, and flow extrusion at the printing starting was referred as group B (see Figure 9).

Figure 9 - Illustration of flow groups



Source: Authors own authorship.

The studied parameters are summarized in Table 3. More samples were made with a same printing parameter for a study in firing in different temperatures, samples for different firing conditions will be referred as temperature sample

Table 3 - Sample's flow arrangement

Sample number	Flow Rate Adjustment (lower)	Flow Rate Adjustment (upper)
1	80	85
2	85	90
3	90	95
4	95	100
5	100	80

Source: Authors own authorship.

This sample arrangement allows the exploration of the flow transitioning during nonstop extrusion.

3.4 GREEN BODY MEASUREMENTS

Green samples dimensions were measured (Axis X, Y and Z) in order to compare the theoretical dimensions set in CAD model using a digital micrometer. Also, mass was measured for comparison to forward processing operations such as the chemical debinding.

The dimensional effectiveness of the printing process was assessed through printing accuracy represented by the calculated linear dimensional change of the as-printed green axis, compared with those of the original CAD model presented by:

$$D_{(i)} = \frac{|l_{CAD} - l_i|}{l_{CAD}} \times 100$$

Where D(i) is deviation, l_{CAD} is the CAD axis length and l_i axis length of the as-printed green samples.

3.5 CHEMICAL DEBINDING

After the printing of the test specimens, chemical extraction and thermal extraction were carried out. The purpose of chemical extraction stage is the partial extraction of binders. This operation focuses on the removal of soluble phases from the feedstock as PW. The batch of chemical extraction for the used feedstock involved immersing the green part in hexane as solvent, heat went from ambient temperature to 65°C for 12 hours, the heating rate proceeded as 0.5°C/min. At the end of this cycle, the part retained its shape and small pores and galleries that were formed from

previous regions filled with PW in the feedstock's polymeric mixture. The Lömi Serie EBA 30 machine, Figure 9, was used for the chemical debinding process.

Figure 10 - Lömi EBA series



Source: Authors own authorship.

3.6 THERMAL DEBINDING

The thermal debinding was done using a muffle furnace (Jung – J 200). The objective of this procedure was to extract thermally the remaining polymeric binder from the samples. The thermal cycle was set as follows: the samples were gradually heated from ambient temperature to 300°C at a heating rate of 2°C/min. Subsequently, the temperature was increased from 300°C to 550°C at a heating rate of 1°C/min. Once the temperature reached 550°C, the samples were held at this temperature for two hours.

3.7 SINTERING

Sintering operations took place in an elevator furnace (1700 Sinter), the flow samples were heated from ambient temperature to 1000°C at 15°C/min heating rate

and from 1000°C to 1500°C in a 10°C/min heating rate. Samples were held at 1500°C for four hours.

The temperature samples were fired in same ascending temperatures and heating rates as FTS until 1500°C. From to 1500°C and beyond the furnace fired at heating rates of 5°C/min. Table 4 describes the firing temperatures in different ramps. All temperature samples were cooled down to ambient temperature with heaters off.

Table 4 - Sample Firing planning

Sample number	Ramp Temperature (°C)	Ramp Time (Hours)
6	1550	4
7	1550	4
8	1575	4
9	1575	4

Source: Authors own authorship

3.8 SAMPLE CHARACTERIZATION

3.8.1 Dimensional Shrinkage

After firing, samples went through dimensional measurement using a digital micrometer (Mitutoyo IP65) as a procedure to analyze shrinkage. Each axis was measured three times in different areas in the axis side.

3.8.2 Scanning Electron Microscope

Samples were cut in half in order to observe the inner defects associated with secondary porosity (see Figure 11). Due to the non-electric conductivity nature of the alumina, the samples were coated with gold through sputtering. The deposited surfaces were grounded with a copper tape. The metal tape will allow the electric connection of the analyzing surface to the metallic support. The Scanning Electron Microscope used was the Tescan – Vega 3.

Figure 11 – Sample prepared for SEM

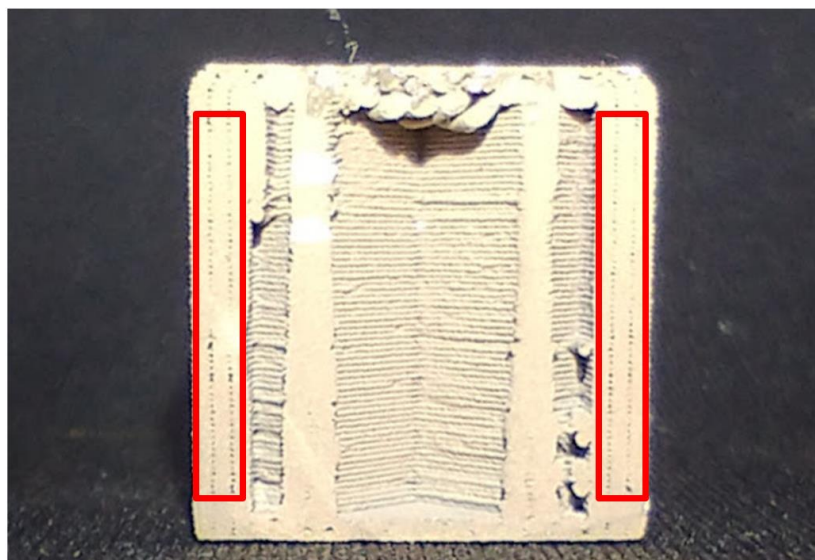


Source: Authors own authorship.

3.9 IMAGE PROCESSING

The obtained images from the scanning electron microscope were processed in MATLAB software to standardize the threshold for void size area. Figure 12 displays the analyzed sample regions, highlighted by the red rectangles. These regions represent the walls set in the printing parameters. As the printing was configured to deposit three walls, there were two intersections.

Figure 12 – Regions containing voids from adjacent deposition

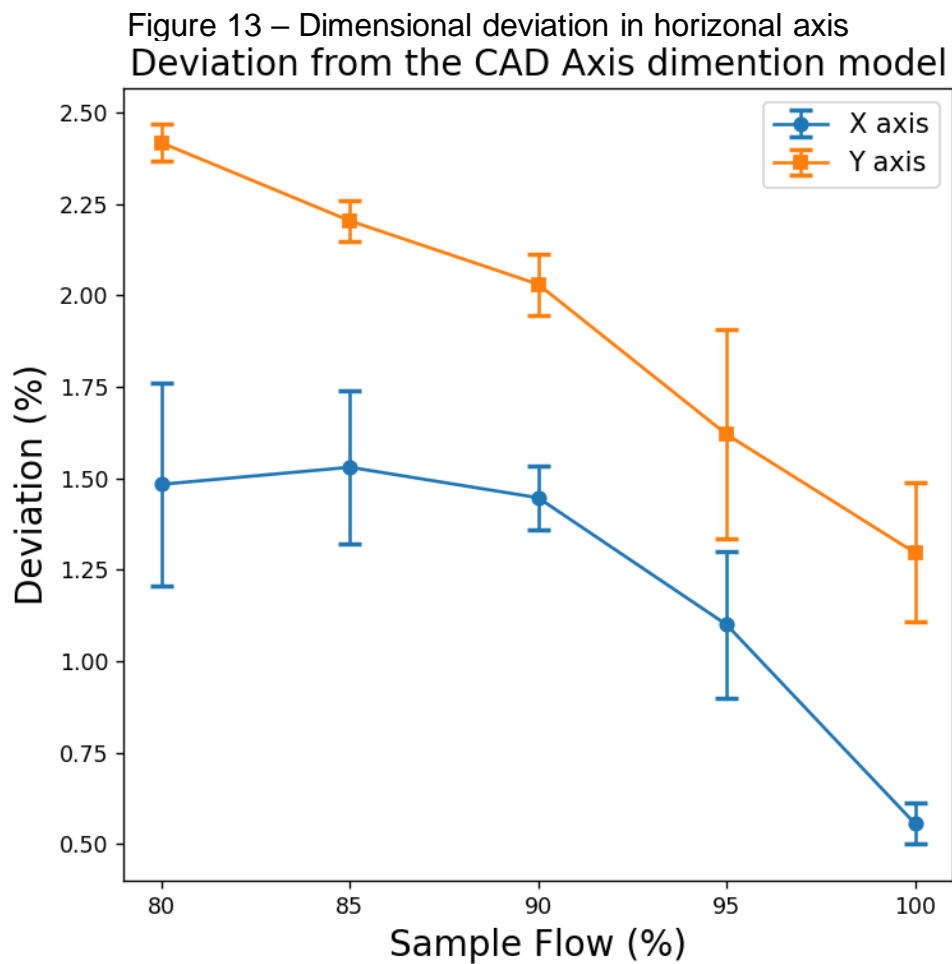


Source: Authors own authorship.

4 RESULTS AND DISCUSSION

4.1 GREEN BODY DIMENSIONAL ACCURACY

The data obtained from the green parts were used to compare their accuracy in comparison with CAD model. The X and Y axes show a trend of decreasing dimensional deviation as the flow increases (see Figure 13).

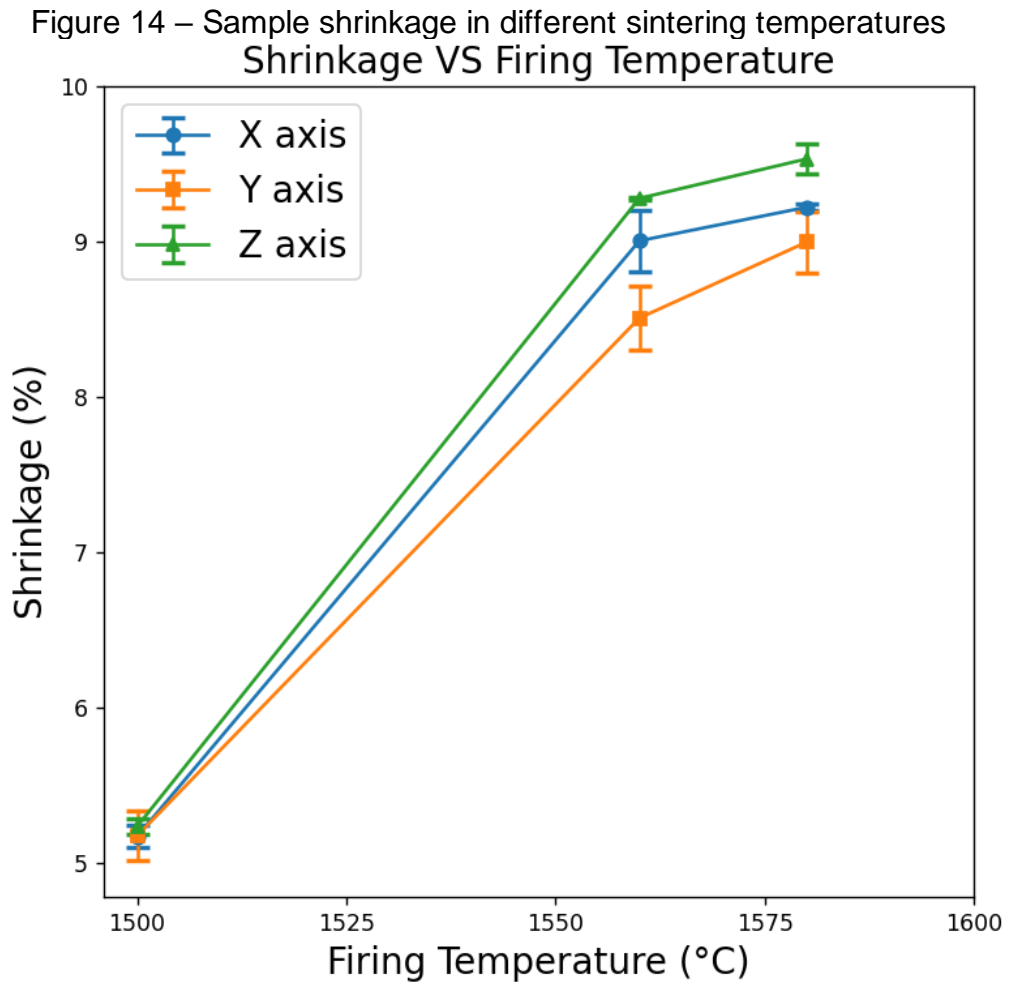


Source: Authors own authorship.

It is noticeable that there is a slight accuracy difference between the axes, with the Y axis demonstrating greater deviation under all flow conditions, ranging from approximately 0.5% to 1%, if compared with the X axis, depending on the flow condition. This divergence can be attributed to the printer's frame and mechanical arrangement, as well as the belt tension in both axes.

4.2 SINTERED BODY MEASUREMENTS

Samples sintered in different temperatures showed different shrinkage (See figure 14). Also, all samples were able to withstand the entire manufacturing operations maintaining their shape in visual inspection.

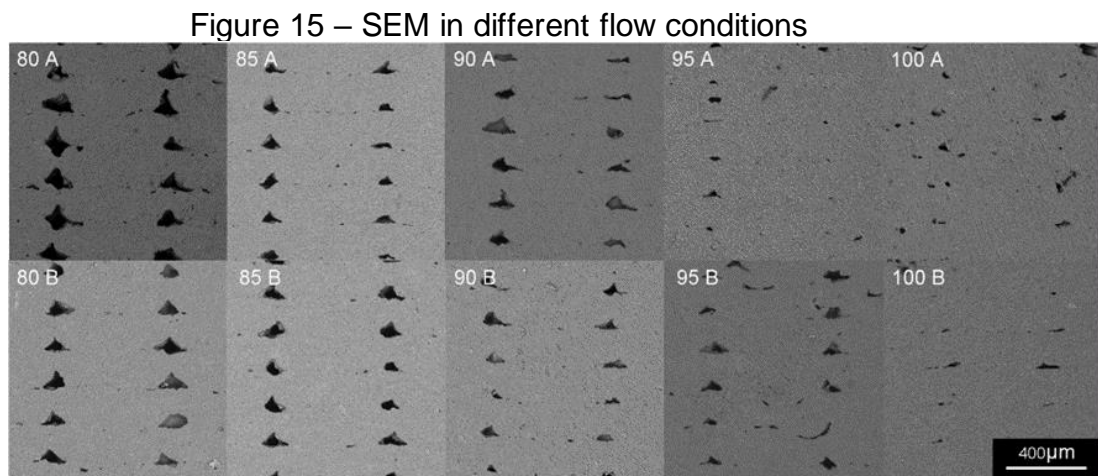


Source: Authors own authorship.

Shrinkage results display a little inconsistency in values between axis. This phenomenon can also be seen in other studies such as ref (ROSNITSCHKEK *et al*, 2021) where results of shrinkage in X and Y showed different behavior of more than 1% in difference between X and Y axis. In the case of Z axis, the influence of the gravity can explain the superior shrinkage compared to X and Y axes

4.3 VOID DEFECTS DUE TO THE EXTRUSION AM PROCESSING

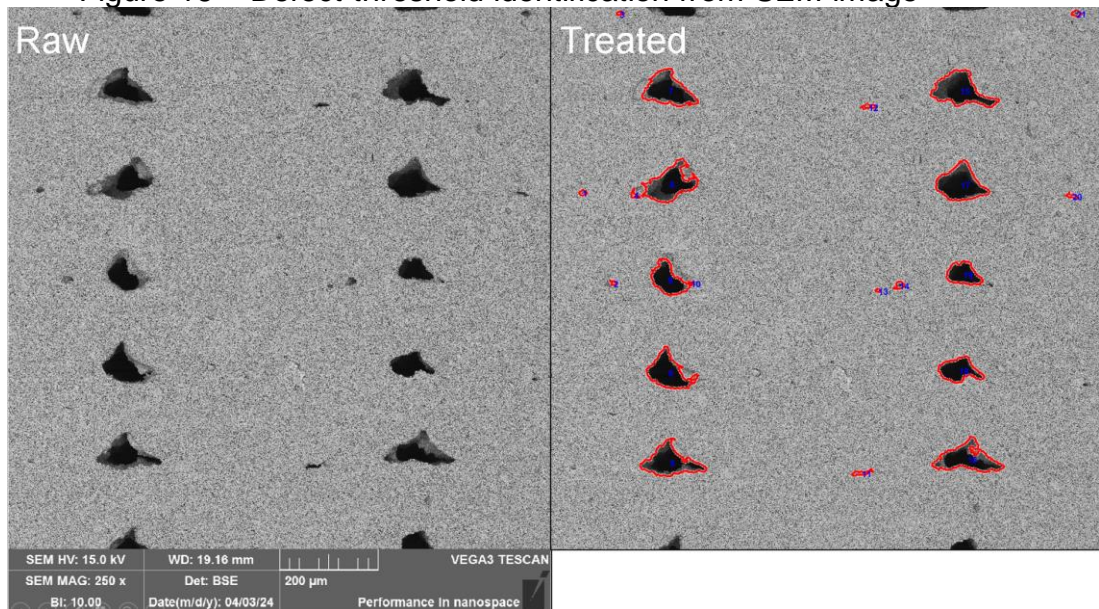
By means of the SEM images (see figure 15), it was possible to identify a trend in defect size influenced by the extrusion flow. The areas of triangle/square-shaped defects were tracked and measured in μm^2 using image's scale as a reference. A relationship between defect area and the corresponding sample's flow can be observed.



Source: Authors own authorship.

Figure 16 displays an example of void defect measurement by image processing of a SEM image sample. The void area was obtained through a thresholding. The void area was computed to generate a mean void size for the given flow condition. Despite the thresholding identification of other types of voids, only voids generated by adjacent extrusion were considered in calculation. From an image sample, the studied voids were computed in order to obtain a mean and a standard deviation of a void size area for the given sample's flow condition.

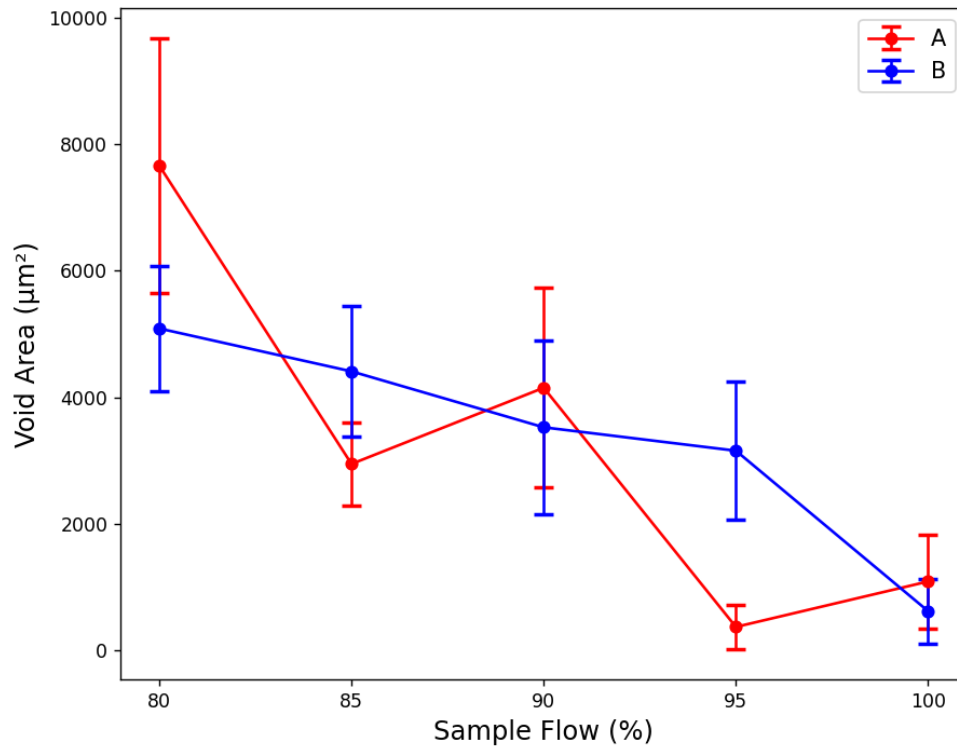
Figure 16 – Defect threshold identification from SEM image



Source: Authors own authorship.

Figure 17 displays a quantification of the flow influence and its relationship with the presence of defects from the thresholding. As mentioned in materials and methods, the group B represented flow condition starting from the printer's base, and the group A represented flow transition change in mid printing. In both scenarios a decreasing trend can be notated as the increase of flow rate led to a reduction of void area.

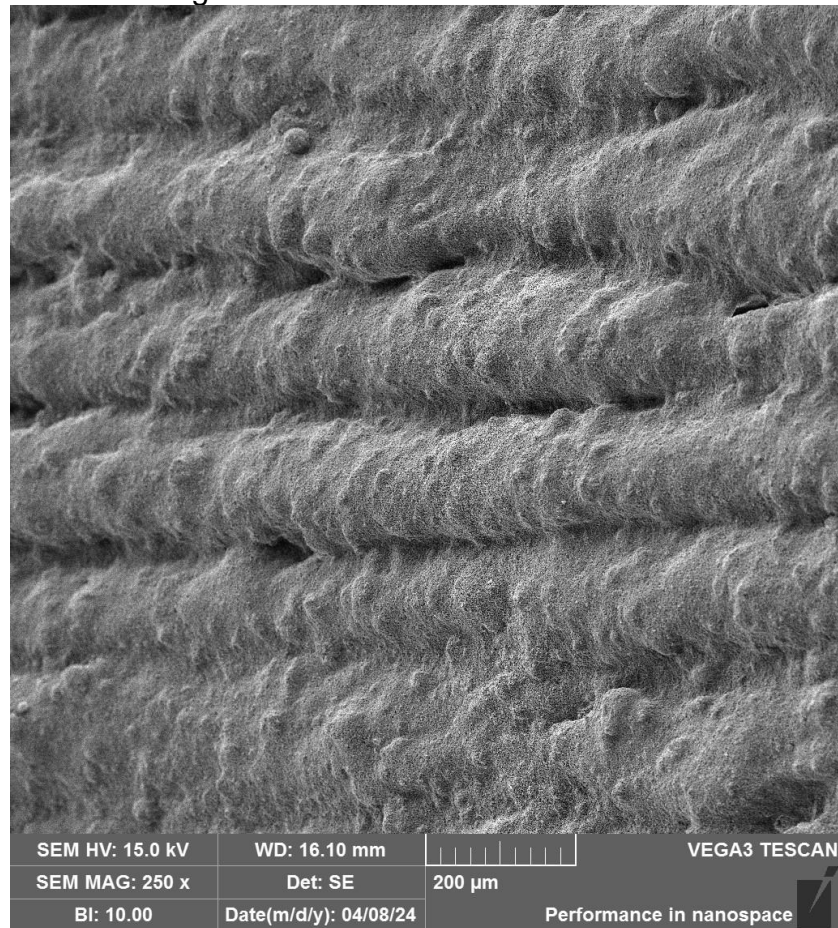
Figure 17 – Void Area in different flow conditions
Void area X Flow



Source: Authors own authorship.

These irregularities can be attributed to shark skin phenomenon (see figure 18), which occurs when the extruding material from the nozzle exhibits a rough, uneven surface. This phenomenon is influenced by viscosity of extruded material, shear rate, temperature, surface interactions between molten feedstock and the nozzle wall, nozzle surface roughness and can significantly impact the surface consistency of the extruded material (GRAHAM, 1999).

Figure 18 – Sintered surface



Source: Authors own authorship.

5 CONCLUSION

This study explored the influence of extrusion flow on the dimensional accuracy, void formation, and surface irregularities in alumina-based feedstock in additive manufacture processing. Key findings are summarized as follows:

5.1 DIMENSIONAL ACCURACY:

The green body measurements indicated a trend of decreasing dimensional deviation with increasing extrusion flow. The Y axis consistently showed greater deviation compared to the X axis, ranging from approximately 0.5% to 1%, which was attributed to the mechanical arrangement and belt tension of the printer.

5.2 SINTERING AND SHRINKAGE:

Samples subjected to different firing temperatures displayed varying degrees of shrinkage, with noticeable inconsistencies between the X and Y axes. This behavior was consistent with other studies and highlights the challenges in achieving uniform shrinkage.

5.3 SECONDARY POROSITY AND SURFACE IRREGULARITIES:

SEM images revealed that defect size decreased with increasing extrusion flow, although this trend was not uniform. The analysis identified that surface irregularities, influenced by the shark skin phenomenon, contributed to these inconsistencies. The shark skin phenomenon contributed for a rough and uneven surface, impacting the overall consistency of the extruded material.

5.4 FUTURE WORK

Overall, the study demonstrated that controlling extrusion flow is critical for optimizing the dimensional accuracy and minimizing void defects in alumina-based additive manufacturing. Future work should focus on refining printer settings and

feedstock composition and further investigating the mechanical and thermal behaviors of the feedstock to enhance the quality and reliability of printed parts.

BIBLIOGRAPHY

ABDULLAHI, A. A.; CHOUDHURY, I. A.; AZUDDIN, M.. Process Development and Product Quality of Micro-Metal Powder Injection Molding. *Materials And Manufacturing Processes*, [S.L.], v. 30, n. 11, p. 1377-1390, 23 mar. 2015. Informa UK Limited. <http://dx.doi.org/10.1080/10426914.2015.1025977>.

ACHILLAS, Charisios; TZETZIS, Dimitrios; RAIMONDO, Maria Olga. Alternative production strategies based on the comparison of additive and traditional manufacturing technologies. *International Journal Of Production Research*, [S.L.], v. 55, n. 12, p. 3497-3509, 31 jan. 2017. Informa UK Limited. <http://dx.doi.org/10.1080/00207543.2017.1282645>.

ALTIPARMAK, Sadettin Cem; YARDLEY, Victoria A.; SHI, Zhusheng; LIN, Jianguo. Extrusion-based additive manufacturing technologies: state of the art and future perspectives. *Journal Of Manufacturing Processes*, [S.L.], v. 83, p. 607-636, nov. 2022. Elsevier BV. <http://dx.doi.org/10.1016/j.jmapro.2022.09.032>.

AMERICAN SOCIETY FOR TESTING AND MATERIALS. ASTM F2792-12A: Standard Terminology for Additive Manufacturing Technologies. West Conshohocken: Astm, 2015.

BALLETTI, Caterina; BALLARIN, Martina; GUERRA, Francesco. 3D printing: state of the art and future perspectives. *Journal Of Cultural Heritage*, [S.L.], v. 26, p. 172-182, jul. 2017. Elsevier BV. <http://dx.doi.org/10.1016/j.culher.2017.02.010>.

BHATIA, Akash; SEHGAL, Anuj Kumar. Additive manufacturing materials, methods and applications: a review. *Materials Today: Proceedings*, [S.L.], v. 81, p. 1060-1067, 2023. Elsevier BV. <http://dx.doi.org/10.1016/j.matpr.2021.04.379>.

BORDIA, Rajendra K.; KANG, Suk-Joong L.; OLEVSKY, Eugene A.. Current understanding and future research directions at the onset of the next century of sintering science and technology. *Journal Of The American Ceramic Society*, [S.L.], v. 100, n. 6, p. 2314-2352, 16 maio 2017. Wiley. <http://dx.doi.org/10.1111/jace.14919>.

CURMI, Albert; ROCHMAN, Arif. From Theory to Practice: development and calibration of micro pellet extruder for additive manufacturing. *Key Engineering Materials*, [S.L.], v. 926, p. 34-45, 22 jul. 2022. Trans Tech Publications, Ltd.. <http://dx.doi.org/10.4028/p-b22a9a>.

DADKHAH, Mehran; TULLIANI, Jean-Marc; SABOORI, Abdollah; IULIANO, Luca. Additive manufacturing of ceramics: advances, challenges, and outlook. *Journal Of The European Ceramic Society*, [S.L.], v. 43, n. 15, p. 6635-6664, dez. 2023. Elsevier BV. <http://dx.doi.org/10.1016/j.jeurceramsoc.2023.07.033>.

DUDA, Thomas; RAGHAVAN, L. Venkat. 3D Metal Printing Technology. *Ifac-Papersonline*, [S.L.], v. 49, n. 29, p. 103-110, 2016. Elsevier BV. <http://dx.doi.org/10.1016/j.ifacol.2016.11.111>.

FILE Optimization Guide. 2024. Disponível em: <https://i.materialise.com/en/learn/file-optimization-guide>. Acesso em: 10 jul. 2024.

GALANTUCCI, Luigi Maria; PELLEGRINI, Alessandro; GUERRA, Maria Grazia; LAVECCHIA, Fulvio. 3D Printing of parts using metal extrusion: an overview of shaping debinding and sintering technology. *Advanced Technologies & Materials*, [S.L.], v. 47, n. 1, p. 25-32, 15 jun. 2022. Faculty of Technical Sciences. <http://dx.doi.org/10.24867/atm-2022-1-005>.

GIBSON, Ian; ROSEN, David W.; STUCKER, Brent. *Additive Manufacturing Technologies: rapid prototyping to direct digital manufacturing*. Berlim: Springer, 2009. 459 p. Disponível em: <https://link.springer.com/book/10.1007/978-1-4419-1120-9#about-this-book>. Acesso em: 10 jul. 2024.

GONZALEZ-GUTIERREZ, Joamin; CANO, Santiago; SCHUSCHNIGG, Stephan; KUKLA, Christian; SAPKOTA, Janak; HOLZER, Clemens. Additive Manufacturing of Metallic and Ceramic Components by the Material Extrusion of Highly-Filled Polymers: a review and future perspectives. *Materials*, [S.L.], v. 11, n. 5, p. 840, 18 maio 2018. MDPI AG. <http://dx.doi.org/10.3390/ma11050840>.

GONZLEZ- GUTIRREZ, Joamn; BEULKE, Gustavo; EMRI, Igor. Powder Injection Molding of Metal and Ceramic Parts. Some Critical Issues For Injection Molding, [S.L.], v. 1, n. 1, p. 66-88, 23 mar. 2012. InTech. <http://dx.doi.org/10.5772/38070>.

GRAHAM, Michael D.. The sharkskin instability of polymer melt flows. Chaos: An Interdisciplinary Journal of Nonlinear Science, [S.L.], v. 9, n. 1, p. 154-163, 1 mar. 1999. AIP Publishing. <http://dx.doi.org/10.1063/1.166386>.

HEIM, Thomas; KERN, Frank. Influence of the Feedstock Preparation on the Properties of Highly Filled Alumina Green-Body and Sintered Parts Produced by Fused Deposition of Ceramic. Ceramics, [S.L.], v. 6, n. 1, p. 241-254, 11 jan. 2023. MDPI AG. <http://dx.doi.org/10.3390/ceramics6010014>.

LAKHDAR, Y.; TUCK, C.; BINNER, J.; TERRY, A.; GOODRIDGE, R.. Additive manufacturing of advanced ceramic materials. Progress In Materials Science, [S.L.], v. 116, p. 100736, fev. 2021. Elsevier BV. <http://dx.doi.org/10.1016/j.pmatsci.2020.100736>.

LAGALA, Andrea; FIORIO, Rudinei; CERETTI, Daniel V. A.; ERKOÇ, Mustafa; CARDON, Ludwig; D'HOOGHE, Dagmar R.. A Combined Experimental and Modeling Study for Pellet-Fed Extrusion-Based Additive Manufacturing to Evaluate the Impact of the Melting Efficiency. Materials, [S.L.], v. 14, n. 19, p. 5566, 25 set. 2021. MDPI AG. <http://dx.doi.org/10.3390/ma14195566>.

LIU, Zengguang; WANG, Yanqing; WU, Beicheng; CUI, Chunzhi; GUO, Yu; YAN, Cheng. A critical review of fused deposition modeling 3D printing technology in manufacturing polylactic acid parts. The International Journal Of Advanced Manufacturing Technology, [S.L.], v. 102, n. 9-12, p. 2877-2889, 7 fev. 2019. Springer Science and Business Media LLC. <http://dx.doi.org/10.1007/s00170-019-03332-x>.

MEDVEDOVSKI, Eugene. Wear-resistant engineering ceramics. Wear, [S.L.], v. 249, n. 9, p. 821-828, set. 2001. Elsevier BV. [http://dx.doi.org/10.1016/s0043-1648\(01\)00820-1](http://dx.doi.org/10.1016/s0043-1648(01)00820-1).

METAL Injection Molding. Disponível em: <https://www.iqsdirectory.com/articles/metal-injection-molding.html>. Acesso em: 10 jul. 2024.

MINTCAD. Why mintcad created its own 3D printing slicer? 2024. Disponível em: <https://medium.com/@mintcad/why-mintcad-created-its-own-3d-printing-slicer-5f6778f83508>. Acesso em: 10 jul. 2024.

MOMENI, V.; ZANGI, H.; ALLAEI, M. H.. Effect of polypropylene as the backbone of MIM feedstock on the micro-structural phase constituents, mechanical and rheological properties of 4605 low alloy steel compacts. *Powder Metallurgy*, [S.L.], v. 63, n. 1, p. 27-34, 12 dez. 2019. SAGE Publications. <http://dx.doi.org/10.1080/00325899.2019.1701812>.

NAKAO, Masayuki; YAN, Chin; YODA, Makoto. MEMS/NEMS. Los Angeles: Springer, 2006. 2142 p. Disponível em: https://link.springer.com/chapter/10.1007/0-387-25786-1_21. Acesso em: 10 jul. 2024.

NÖTZEL, Dorit; EICKHOFF, Ralf; HANEMANN, Thomas. Fused Filament Fabrication of Small Ceramic Components. *Materials*, [S.L.], v. 11, n. 8, p. 1463, 17 ago. 2018. MDPI AG. <http://dx.doi.org/10.3390/ma11081463>.

OLHERO, S.M.; TORRES, P.M.C.; MESQUITA-GUIMARÃES, J.; BALTAZAR, J.; PINHO-DA-CRUZ, J.; GOUVEIA, S.. Conventional versus additive manufacturing in the structural performance of dense alumina-zirconia ceramics: 20 years of research, challenges and future perspectives. *Journal Of Manufacturing Processes*, [S.L.], v. 77, p. 838-879, maio 2022. Elsevier BV. <http://dx.doi.org/10.1016/j.jmapro.2022.02.041>.

PEREIRA, Gabriel K.R.; GUILARDI, Luís F.; DAPIEVE, Kiara S.; KLEVERLAAN, Cornelis J.; RIPPE, Marília P.; VALANDRO, Luiz Felipe. Mechanical reliability, fatigue strength and survival analysis of new polycrystalline translucent zirconia ceramics for monolithic restorations. *Journal Of The Mechanical Behavior Of Biomedical Materials*, [S.L.], v. 85, p. 57-65, set. 2018. Elsevier BV. <http://dx.doi.org/10.1016/j.jmbbm.2018.05.029>.

ROSNITSCHKEK, Tobias; SEEFELDT, Andressa; ALBER-LAUKANT, Bettina; NEUMEYER, Thomas; ALTSTÄDT, Volker; TREMMEL, Stephan. Correlations of Geometry and Infill Degree of Extrusion Additively Manufactured 316L Stainless Steel Components. *Materials*, [S.L.], v. 14, n. 18, p. 5173, 9 set. 2021. MDPI AG. <http://dx.doi.org/10.3390/ma14185173>.

SINGH, Sunpreet; RAMAKRISHNA, Seeram; BERTO, Filippo. 3D Printing of polymer composites: a short review. *Material Design & Processing Communications*, [S.L.], v. 2, n. 2, p. 1-13, 26 ago. 2019. Hindawi Limited. <http://dx.doi.org/10.1002/mdp2.97>.

THOMAS-VIELMA, P.; CERVERA, A.; LEVENFELD, B.; VÁREZ, A.. Production of alumina parts by powder injection molding with a binder system based on high density polyethylene. *Journal Of The European Ceramic Society*, [S.L.], v. 28, n. 4, p. 763-771, jan. 2008. Elsevier BV. <http://dx.doi.org/10.1016/j.jeurceramsoc.2007.08.004>.

TUELUEMEN, Metin; HANEMANN, Thomas; HOFFMANN, Michael J.; OBERACKER, Rainer; PIOTTER, Volker. Process Development for the Ceramic Injection Molding of Oxide Chopped Fiber Reinforced Aluminum Oxide. *Key Engineering Materials*, [S.L.], v. 742, p. 231-237, 3 jul. 2017. Trans Tech Publications, Ltd.. <http://dx.doi.org/10.4028/www.scientific.net/kem.742.231>.

ZAKY, Magdy Tadrous. Effect of solvent debinding variables on the shape maintenance of green molded bodies. *Journal Of Materials Science, Cairo*, v. 39, n. 1, p. 3397-3402, jan. 2004.

ZHAO, Peng; ZHANG, Jianfeng; DONG, Zhengyang; HUANG, Junye; ZHOU, Hongwei; FU, Jianzhong; TURNG, Lih-Sheng. Intelligent Injection Molding on Sensing, Optimization, and Control. *Advances In Polymer Technology*, [S.L.], v. 2020, p. 1-22, 31 mar. 2020. Hindawi Limited. <http://dx.doi.org/10.1155/2020/7023616>.

ZOCCA, Andrea; COLOMBO, Paolo; GOMES, Cynthia M.; GÜNSTER, Jens. Additive Manufacturing of Ceramics: issues, potentialities, and opportunities. *Journal Of The*

American Ceramic Society, [S.L.], v. 98, n. 7, p. 1983-2001, jul. 2015. Wiley.
<http://dx.doi.org/10.1111/jace.13700>.